




Vector Aided Microenvironment programming (VAMP): reprogramming the TME with MVA virus expressing IL-12 for effective antitumor activity

Laura Secli ¹, Luigia Infante^{1,2}, Linda Nocchi ¹, Maria De Lucia,¹ Gabriella Cotugno,¹ Guido Leoni,¹ Elisa Micarelli,¹ Irene Garzia,¹ Lidia Avalle,³ Giulia Sdruscia,¹ Fulvia Troise,¹ Simona Allocca,¹ Giuseppina Romano,¹ Elisa Scarselli,¹ Anna Morena D'Alise ¹

To cite: Secli L, Infante L, Nocchi L, *et al.* Vector Aided Microenvironment programming (VAMP): reprogramming the TME with MVA virus expressing IL-12 for effective antitumor activity. *Journal for ImmunoTherapy of Cancer* 2023;**11**:e006718. doi:10.1136/jitc-2023-006718

► Additional supplemental material is published online only. To view, please visit the journal online (<http://dx.doi.org/10.1136/jitc-2023-006718>).

LS and LI contributed equally.
Accepted 11 April 2023



© Author(s) (or their employer(s)) 2023. Re-use permitted under CC BY-NC. No commercial re-use. See rights and permissions. Published by BMJ.

¹NousCom, Rome, Italy

²University of Rome Tor Vergata, Roma, Lazio, Italy

³Department of Molecular Biotechnology and Health Science, University of Turin, Torino, Piemonte, Italy

Correspondence to

Dr Anna Morena D'Alise;
m.dalise@nouscom.com

ABSTRACT

Background Tumor microenvironment (TME) represents a critical hurdle in cancer immunotherapy, given its ability to suppress antitumor immunity. Several efforts are made to overcome this hostile TME with the development of new therapeutic strategies modifying TME to boost antitumor immunity. Among these, cytokine-based approaches have been pursued for their known immunomodulatory effects on different cell populations within the TME. IL-12 is a potent pro-inflammatory cytokine that demonstrates striking immune activation and tumor control but causes severe adverse effects when systemically administered. Thus, local administration is considered a potential strategy to achieve high cytokine concentrations at the tumor site while sparing systemic adverse effects.

Methods Modified Vaccinia Ankara (MVA) vector is a potent inducer of pro-inflammatory response. Here, we cloned IL-12 into the genome of MVA for intratumoral immunotherapy, combining the immunomodulatory properties of both the vector and the cargo. The antitumor activity of MVA-IL-12 and its effect on TME reprogramming were investigated in preclinical tumor models. RNA sequencing (RNA-Seq) analysis was performed to assess changes in the TME in treated and distal tumors and the effect on the intratumoral T-cell receptor repertoire.

Results Intratumoral injection of MVA-IL-12 resulted in strong antitumor activity with the complete remission of established tumors in multiple murine models, including those resistant to checkpoint inhibitors. The therapeutic activity of MVA-IL-12 was associated with very low levels of circulating cytokine. Effective TME reprogramming was demonstrated on treatment, with the reduction of immunosuppressive M2 macrophages while increasing pro-inflammatory M1, and recruitment of dendritic cells. TME switch from immunosuppressive into immunostimulatory environment allowed for CD8 T cells priming and expansion leading to tumor attack.

Conclusions Intratumoral administration of MVA-IL-12 turns immunologically 'cold' tumors 'hot' and overcomes resistance to programmed cell death protein-1 blockade.

WHAT IS ALREADY KNOWN ON THIS TOPIC

⇒ Interleukin (IL)-12 is a potent pro-inflammatory cytokine in the tumor microenvironment, able to control tumor growth, favoring immune activation but causes severe adverse effects when systemically administered.

WHAT THIS STUDY ADDS

⇒ In this study, we propose a novel approach based on the use of Modified Vaccinia Ankara (MVA) vector encoding IL-12 for intratumoral delivery, combining the safety profile of MVA and its pro-inflammatory properties with the strong immunostimulatory function of IL-12 in combination with α -programmed cell death protein-1, for effective antitumor response while sparing systemic adverse effects due to IL-12 circulating levels.

HOW THIS STUDY MIGHT AFFECT RESEARCH, PRACTICE OR POLICY

⇒ This study highlights the potential of MVA-IL-12 for the treatment of solid tumors resistant to immunotherapy.

BACKGROUND

Despite the great success of immunotherapy as a beneficial tool for cancer treatment, the efficacy of immune checkpoint inhibitors (CPI) is unfortunately restricted to a limited number of patients.¹ The differences in the outcome of cancer immunotherapy are often attributed to the tumor microenvironment (TME) that can play an opposite role both in tumor immune surveillance or in immunological evasion.^{2,3} TME consists of tumor cells, cancer-associated fibroblasts, the tumor vasculature, the extracellular matrix and the immune cells, including T and B lymphocytes, tumor-associated macrophages (TAM), dendritic cells (DC), natural killer (NK), neutrophils and myeloid-derived suppressor

cells (MDSC). In this milieu, cytokines, released by cancer cells and by TME components, are key players to generate feedback loop that can promote tumor transformation, protect the tumor from host immunity, support tumor growth and invasion, foster therapeutic resistance and provide niches for dormant metastases to thrive.⁴

Therefore, multiple strategies to overcome resistance and therapeutically target the TME have been developed, including depletion of cancer-promoting cells or their re-education toward immune stimulating, tumor suppressive phenotypes.⁵ Recently, numerous clinical trials have been conducted to investigate the potential antitumor activity of a number of recombinant cytokines that can generate a potent and coordinated immune response against cancer cells, turning immunologically 'cold' tumors to 'hot'.⁵ Intratumoral (IT) administration represents a valuable and promising therapeutic option to develop potentially more effective and less toxic immunotherapies, including cytokines-based therapies. Given the several advantages of local immunotherapy, a plethora of agents are currently tested with intratumoral injections in clinical trials, including monoclonal antibodies, cytokines, non-oncolytic and oncolytic viral therapies.⁶

Interleukin (IL)-12, a potent pro-inflammatory cytokine, normally produced by antigen presenting cells, bridges the innate and adaptive immune systems.⁷ Belonging to a family of heterodimeric cytokines, IL-12 is comprised of two subunits, p35 and p40, linked by three disulfide bridges to form a p70 heterodimer.^{8,9} Among its different functions, IL-12 is responsible for the induction and enhancement of cell-mediated immunity: induces TH1 cell differentiation,^{10–12} increases activation and cytotoxic capacities of T and NK cells^{13,14} and inhibits or reprograms immunosuppressive cells, such as TAMs.^{15–18} Not surprisingly, although IL-12 has demonstrated robust antitumor activity in preclinical studies, its systemic administration has been shown to be exceedingly toxic, inducing the production of large amounts of interferon (IFN)- γ , which is cytostatic and cytotoxic. For this reason, localized delivery strategies are needed to enhance IL-12 concentrations in the TME and decrease systemic toxicity.^{19–21}

To this aim, we developed a novel approach of 'Vector Aided Microenvironment programming: VAMP' to turn immunologically 'cold' tumors 'hot', with the generation of Modified Vaccinia virus Ankara (MVA) encoding IL-12. MVA is a highly attenuated poxvirus unable to replicate in most mammalian cells, originally developed in the 1970s as a vaccine against smallpox. Moreover, MVA has been recently approved as a vaccine against monkeypox.^{22–23} The virus has unimpaired expression of early and intermediate genes as well as most late genes but its replication cycle is blocked at a very late stage and thus cannot produce infectious progeny and spread after vaccination. Since the replication defect occurs at a late stage of virion assembly, MVA is still able to efficiently express viral genes, including encoded genes (vaccine antigens or immunomodulatory molecules).²⁴ Due to its favorable

safety profile, MVA has been used in a number of clinical trials for infectious disease and cancer and no serious adverse events were reported until now.^{24–29}

In this study, we coupled the immunostimulatory properties of MVA and its safe profile with the pro-inflammatory function of IL-12 by generating an MVA encoding IL-12 for IT administration to remodel TME and enhance antitumor response in both CPI sensitive and resistant tumor models. We demonstrated that IT injection of MVA-IL-12 exerts strong therapeutic responses in various tumor models, alone and in combination with α -programmed cell death protein-1 (α PD-1). Therapeutic activity of IT MVA-IL-12 is associated with recruitment of conventional type 1 DC (cDC1), reduction of immunosuppressive M2 macrophages, increase of pro-inflammatory M1 macrophages and CD8 T effectors in the tumor. Our data strongly support the use of MVA-IL-12 as a novel strategy to overcome TME-mediated resistance to immunotherapy.

METHODS

Viruses

For generation of MVA-mIL-12 vectors, single chain murine IL-12 transgene³⁰ was synthesized by GeneART (Thermo Fisher Scientific) and subcloned into shuttle plasmid green (same as described³¹) but with a synthetic early/late promoter driving transgene expression via BamHI/AscI restriction enzymes (New England Biolabs). The transgene cassette was transferred into the Deletion III locus of MVA by homologous recombination in AGE1. CR.pIX cells (ProBioGen, Berlin, Germany). Recombinant MVA were isolated by combination of marker gene swapping and fluorescence-activated cell sorting as previously reported³¹ followed by a limiting dilution step to obtain a pure viral population. The obtained recombinant vectors were amplified by infecting eight T175 flasks of chicken embryo fibroblasts (CEF) at not controlled Multiplicity of Infection (MOI). Infected cells were collected at full cytopathic effect (CPE) and centrifuged for 1 hour at 24,000g; the resulting pellet was resuspended in 10 mM Tris-HCl pH 9.0 and cells lysed by three cycles of freeze/thaw followed by 5' sonication (max amplitude, Bioruptor Plus, Diagenode) and passage through a syringe with a 26G needle. Cell debris were pelleted at 1800g for 5', and supernatant loaded on 15 mL of 36% Sucrose in 10 mM Tris-HCl pH 9.0 and centrifuged for 1 hour at 30,000g at 4°C. The obtained virus pellet was resuspended in 140 mM NaCl, 10 mM Tris pH 7.7, sonicated for 10' (Bioruptor Plus, Diagenode), filtered through 0.45 μ m syringe filters and stored at -80°C. No DNA digestion steps were performed during purification process nor the virus was tested for Mycoplasma. The sequence is indicated in online supplemental material.

Cell cultures

The MC38 (murine C57BL/6 colon adenocarcinoma) cell line, the CT26 (murine BALB/c colorectal

carcinoma) cell line, the B16F10 (murine C57BL/6 melanoma) cell line and the HeLa cell line were purchased from American Type Culture Collection (ATCC). MC38 and B16F10 cells were maintained in Dulbecco's Modified Eagle Medium (DMEM) (Gibco, cat. 41966052), supplemented with heat-inactivated 10% fetal bovine serum (FBS) (Gibco, cat. 26140079), 1% (v/v) penicillin/streptomycin (Gibco, cat. 15140122); CT26 cells were cultured in Roswell Park Memorial Institute (RPMI) 1640 medium (Gibco, cat. 21875091), supplemented with heat-inactivated 10% FBS and 1% (v/v) penicillin/streptomycin. HeLa cells were maintained in Eagle's Minimum Essential Medium (EMEM) (ATCC, cat. 30–2003) supplemented with heat-inactivated 10% FBS and 1% (v/v) penicillin/streptomycin. Cell lines were maintained at 37°C in 5% CO₂ and routinely tested for mycoplasma contamination by PCR.

Mice

Six-week-old female C57BL/6 and BALB/c mice were purchased from Envigo. Daily animal care was performed by trained mouse house staff at Plaisant, Castel Romano. All experimental procedures were approved by the Italian Ministry of Health (Authorizations 213/2016 PR) and have been done in accordance with the applicable Italian laws (D.L.vo 26/14 and following amendments), the Institutional Animal Care and Allevamenti Plaisant SRL. Six-week-old B6.129S(C)-Batf3tm1Kmm/J and 6-week-old female C57BL/6 mice (Charles River Laboratories) were kept in pathogen-free conditions in the animal facility of the Molecular Biotechnology Center (University of Turin). Experiments with mice were carried out in accordance with the ethical guidelines of the European Communities Council Directive (2010/63/EU). Experimental approval was obtained from the Italian Health Ministry (673/2022-PR).

In vivo studies

For established tumor setting experiments, 2×10^5 MC38 or 5×10^5 B16F10 cells were subcutaneous (SC), injected into the right flank of C57BL/6 mice. In dual tumor models 2×10^5 MC38 cells were implanted in the right flank (treated tumor) and 1×10^5 MC38 cells in the left flank (distant). After 7 days, at day 0, tumor mass was measured with a digital caliper, applying the formula: $a \times b/2$, where $a < b$. Animals were then randomized based on their tumor size (tumor size average per group ~ 50 – 100 mm³) and started to receive treatments based on the study. Animal survival was monitored for the entire experiment and tumor growth was measured every 3–4 days and mice were euthanized as soon as signs of distress or a tumor volume above 1500 mm³ was reached. For intraperitoneal (IP) tumor challenge BALB/c mice were administered with 3×10^5 CT26 in the peritoneum. Mice were weighted and randomized into their respective groups 3 days after tumor challenge. Animal survival was monitored for the entire experiment and weight was measured every 3–4 days. Mice were euthanized when they gained >20%

of initial weight or when they displayed other signs of distress (eg. pallor, lethargy, poor mobility, poor feeding, poor ambulation). For re-challenge experiments, tumor-free and surviving animals were re-challenged SC or IP with parental tumor cell line (in the same amount of the first challenge).

In vivo drug administration

Schematic representation of each experiment is shown in figures. MVA empty or MVA-IL-12 were prepared at the desired concentration (6×10^5 Infectious Unit, IFU or 10^7 IFU) in phosphate-buffered saline (PBS) to a final volume of 50 μ l and administered by IT injection in anesthetized mice or to a final volume of 100 μ l and administered by IP injection. Murine α PD-1 (Bio X Cell, clone RMP114, cat. BE0146) was administered IP at a dosage of 200 μ g two times per week, starting from day 0 until day 21. For immune depletion studies murine α CD4 (Bio X Cell, clone GK1.5, cat. BE0119), α CD8 (Bio X Cell, clone YTS 169.4, cat. BE0117) or anti rat IgG2b Isotype Control (Bio X Cell, clone LTF-2, cat. BE0090) were administered IP at a dosage of 200 μ g every 4 days, starting from day 0, for a total of five administrations. For NK depletion murine α NK1.1 (Bio X Cell, clone PK136, cat. BE0036) was administered IP at a dosage of 200 μ g at day -2, 3, 8, 12 as described in Kirchhammer *et al*, 2022.³² Mice were checked daily for adverse clinical reactions.

Flow cytometry

Murine tumors were dissociated mechanically with lancet and then using the tumor tissue dissociation kit (Miltenyi Biotec, cat. 130-096-730). Tumor homogenates were then depleted from erythrocytes using ACK Lysing Buffer (Gibco, cat. A1049201), washed in Fluorescence-Activated Cell Sorter (FACS) buffer (1 \times PBS, 0.5% FBS) and filtered through a 70 μ m cell strainer to generate single-cell suspension. For analysis of the peritoneal cavity cells, peritoneal lavage of mice was performed by infusing 5 mL of cold PBS intraperitoneally and collecting the infusate as described by Ray and Dittel.³³ Samples were incubated with anti-mouse CD16/32 (BD, clone 2.4G2, cat. 553142) 1:50 in FACS buffer for 20' at 4°C. After washing with PBS, samples were stained with LIVE/DEAD Fixable Near-IR Dead Cell Stain Kit (Thermo Fisher Scientific, L10119) 1:100 in PBS for 20' at room temperature (RT) in the dark. After washing with FACS buffers, samples were stained for surface antigens in FACS buffer for 30' at RT in the dark. Foxp3 intracellular staining was performed following the instructions of Foxp3/Transcription Factor Staining Buffer Set (eBioscience, cat. 00-5523-00). IFN- γ intracellular staining was performed following the instructions of Fixation/Permeabilization Kit (BD, cat. 554714). Myeloid compartment: CD45 (BD, clone 30-F11, cat. 563891), CD11b (BioLegend, clone M1/70, cat. 101206), F480 (BioLegend, clone BM8, cat. 123113), Ly6C (BioLegend, clone hk1.4, cat. 128012), Ly6G (BioLegend, clone 1A8, cat. 127614), MHCII (BioLegend, clone M5/114.15.2, cat. 107632), CD206

(BioLegend, clone C068C2, cat. 141706). Lymphoid compartment: CD3 (BioLegend, clone 145-2C11, cat. 100312), CD4 (BioLegend, clone RM 4-5, cat. 100512), CD8 (BioLegend, clone 53-6.7, cat. 100732), CD19 (BD, clone 1D3, cat. 553785). Treg: CD45 (eBioscience, clone 30-F11, cat. 45-0451-82), CD4 (BioLegend, clone RM 4-5, cat. 100531), CD8 (BioLegend, clone 53-6.7, cat. 100752), Foxp3 (eBioscience, clone FJK-16s, cat. 17-5773-82). CD8 memory subpopulations: CD8 (BioLegend, clone 53-6.7, cat. 100752), CD44 (BioLegend, clone IM7, cat. 103022). Dendritic Cells: CD14 (BioLegend, clone Sa14-2, cat. 123314), CD11c (BioLegend, clone n418, cat. 117310) or MHCII (BioLegend, clone M5/114.15.2, cat. 107626), CD11b (BioLegend, clone M1/70, cat. 101206), CD8 (BioLegend, clone 53-6.7, cat. 100752), CD103 (BioLegend, clone 2E7, cat. 121426), XCR1 (BioLegend, clone ZET, cat. 148216), SIRP/CD172 (BioLegend, clone P84, cat. 144012). Natural killer: CD45 (BioLegend, clone 30-F11, cat. 103137), CD3 (BioLegend, clone 145-2C11, cat. 100312), CD49b (BioLegend, clone DX5, cat. 553858), NK-1.1 (BioLegend, clone PK136, cat. 108732).

Circulating and tumor cytokine measurement

Murine tumors were weighted and then minced with lancet. The T-PER Tissue Protein Extraction Reagent (Thermo Fisher Scientific, cat. 78510) was used as a homogenizing buffer for the tumors (500 µl of T-PER per 100 mg of tissue) in presence of protease inhibitors (Thermo Fisher Scientific, cat. 78437). Dissociation by tissue lyser was performed for 5' at 30 Hz; then samples were centrifuged at 10,000 g for 30' at 4°C. Supernatant was collected, proteins were quantified with Bio-Rad Protein Assay Kits (Bio-Rad, cat. 5000006) and 1 µg was loaded in each well. Murine bleed or cell supernatants were centrifuged at 12,500 g for 5' at RT and the supernatant was collected. For the analysis of murine IL-12 was used the IL-12 p70 Mouse ELISA Kit (Thermo Fisher Scientific, cat. BMS6004) following the kit instructions.

Gene expression analysis

RNA was extracted from tumor samples (AllPrep DNA/RNA Micro Kit, Qiagen, cat. 80284). Next Generation Sequencing (NGS) of tumor samples was performed at CeGat GmbH. RNA was subject to initial quality control. During the library preparation ribosomal RNA was depleted and total RNA was analyzed and sequenced on the Illumina platform (NovaSeq 6000, Read length 2×100 bp, output 50M clusters (10 Gb) per sample). Raw NGS reads were aligned on the mm10 genome by using hisat2 software.³⁴ Differentially expressed genes (DEGs) were determined by using four alternative methods: Deseq2,³⁵ EdgeR,³⁶ limma with Voom correction³⁷ and NOISeq.³⁸ Each method was applied to a count matrix reporting the number of reads mapped to each gene as estimated by the Rsubread package.³⁹ For each comparison, we retained only genes identified by the consensus of three out of four methods, with a log₂FC of at least ±1 and a Benjamini-Hochberg corrected p value ≤ 0.05.

Only the DEGs with <10 total count of mapped reads in all samples in at least one condition and expressed with a median Transcripts per Million (TPM) ≥ 1 in at least one of the compared condition were retained.

After RNA extraction with AllPrep DNA/RNA Micro Kit, Qiagen, cat. 80284, 1 µg of RNA was retro-transcribed with SuperScript First-Strand Synthesis System (Thermo Fisher Scientific, cat. 11904018) following the instructions. RT-PCR was performed with TaqMan Universal PCR Master Mix (Applied Biosystems, cat. 4304437) and the following probes (Best coverage, Probe spans exons, FAM, cat. 4453320): Actin Mm00607939_s1, Ccl5 Mm01302427_m1, CD86 Mm00444540_m1, Clec17a Mm01183349_m1, Cxcl9 Mm00434946_m1, Granzyme B Mm00442837_m1, H2-Ab1 Mm00439216_m1, Ifnγ Mm01168134_m1, Il7r Mm00434295_m1, Itgb2 Mm00434513_m1, Nos2 Mm00440502_m1, Perforin 1 Mm00812512_m1.

Intratumoral TCR repertoire

TCR repertoire was characterized by reconstructing T-cell receptor β-chains from whole tissue RNA-Seq. The derived CDR3 sequences were further analyzed by tracking the expansion of clonotypes among different treatments.

Statistical analysis

The data are presented as mean ± SEM. For statistical analyzes, significance was tested using the Student's t-test, one-way analysis of variance (ANOVA), and two-way ANOVA with Fisher least significant difference post hoc test. A minimum value of p < 0.05 was considered statistically significant. Statistical analyzes were performed using GraphPad Prism V.9.

RESULTS

Intratumoral treatment with MVA-mIL-12 is highly effective alone and in combination with αPD-1 in CPI sensitive and resistant model

The expression of MVA encoded mIL-12 (MVA-mIL-12) (figure 1A) was first evaluated in vitro, by ELISA assay on HeLa cells infected at MOI 5 and analyzed at different time points post infection, compared with mock infected cells (figure 1B) showing a good expression levels detected over-time. The levels and kinetic of expression of the encoded mIL-12 were then confirmed in vivo on intratumoral injection of MVA-mIL-12 (6×10⁵ IFU) in MC38 tumor bearing mice (figure 1C). Blood and tumors were collected at different time points and ELISA assay was performed to quantify the level of mIL-12 protein. In tumors, the peak of IL-12 was observed at 6-hour post injection, with a complete drop of the protein at 96 hours (figure 1C). Serum IL-12 levels were also detected on intratumoral injection, likely due to secretion of the cytokine from the tumor into the periphery. These serum levels quickly became almost undetectable 48 hours post IT injection, supporting a favorable pharmacokinetics (PK) profile.

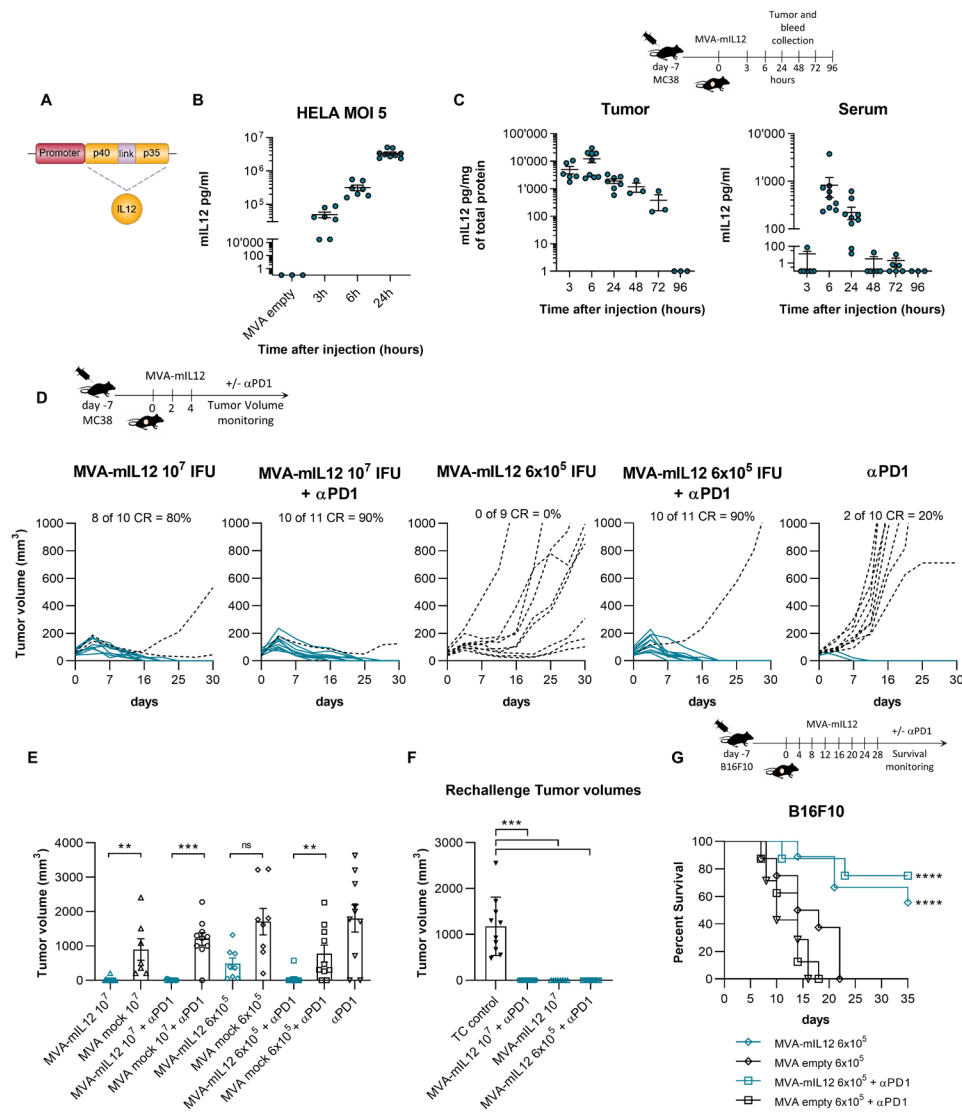


Figure 1 Potent efficacy of intratumoral MVA-mIL-12 in different syngeneic preclinical models. (A) Schematic structure of MVA-mIL-12. (B) HeLa cells were infected at MOI 5 with MVA-mIL-12 or MVA empty and supernatants were collected at different time points to quantify IL-12 by ELISA. (C) In vivo levels of IL-12. C57BL/6 mice were challenged subcutaneously (SC) with MC38 cells. After 7 days, mice with established tumors were randomized, treated intratumoral (IT) with MVA-mIL-12 (6×10^5 IFU), and serum was collected at different time points post injection. The amount of IL-12 was measured by ELISA in tumor tissue and serum ($n \geq 3$). (D) C57BL/6 mice were challenged SC with MC38 cells. After 7 days, mice with established tumors were randomized and treated IT three times with MVA-mIL-12 at 10^7 IFU alone or in combination with α -PD-1, with MVA-mIL-12 at 6×10^5 IFU alone or in combination with α -PD-1 as control. Tumor volume was monitored over time. Lines in the graphs represent each individual tumor (full lines, responder tumors showing a complete response (CR); dot lines, non-responder tumors). Percentages on the graphs indicate the rate of CR. (E) Tumor volumes are shown as mean \pm SEM with $n \geq 6$ (day 25). (F) Mice considered complete responders were re-challenged with MC38, 40 days after tumor challenge. Tumor volumes post re-challenge are shown as mean \pm SEM with $n = 10$. One-way ANOVA test with Fisher's LSD test was performed to obtain p value. (G) Survival curves of C57BL/6 mice SC injected with B16F10 cells. After 7 days, mice with established tumors were randomized and treated IT eight times with MVA-mIL-12 at 6×10^5 IFU or MVA empty at 6×10^5 IFU alone or in combination with α -PD-1 or α -PD-1 as control. $n \geq 6$. Comparison of survival curves with Gehan-Breslow-Wilcoxon test. *, $p < 0.05$; ***, $p < 0.001$; ****, $p < 0.0001$. ANOVA, analysis of variance; IFU, Infectious Unit; IL, interleukin; LSD, least significant difference; m, murine; MOI, Multiplicity of Infection; MVA, Modified Vaccinia virus Ankara; ns, not significant; PD-1, programmed cell death protein-1.

The therapeutic potential of MVA-mIL-12 was explored in the CPI responsive murine model of MC38. Cancer cells were subcutaneously injected in mice and, after tumor establishment, MVA-mIL-12 was administered three times IT at day 0, 2 and 4 at two different doses, 6×10^5 IFU and a 20-fold higher dose of 10^7 IFU, in

presence or absence of α PD-1 (figure 1D). The dose of 6×10^5 IFU corresponds to a human equivalent dose of $\sim 2 \times 10^9$ IFU that falls in the range of MVA dosages already used in humans. Treatment with α PD-1 alone was effective only in curing 20% of mice. MVA-mIL-12 monotherapy

at 6×10^5 IFU controlled tumor growth with shrinkages of the tumor masses observed in some cases but without reaching complete tumor eradication; the combination of MVA-mIL-12 (6×10^5 IFU) and α PD-1 resulted in 90% of cure, demonstrating a significant improvement over the α PD-1 monotherapy and complete tumor eradication in the majority of mice (figure 1D). The higher dose of 10^7 IFU resulted in more effective antitumor activity as monotherapy, with 80% of complete responses in treated mice. However, the combination of MVA-mIL-12 (10^7 IFU) with α PD-1 was not found to be significantly superior to the lower dose (figure 1D), with 90% of cure observed post treatment. No effect was observed on tumors treated with MVA empty (at different doses) as monotherapy, while the combination of MVA empty with α PD-1 was comparable to α PD-1 (figure 1E and online supplemental figure 1A). The reduction of the number of injections to one and two administrations was less effective (online supplemental figure 1B). Complete responder mice were resistant to tumor re-challenge with MC38 cells (figure 1F) demonstrating the development of immunological memory.

To assess the efficacy of MVA-mIL-12 in CPI resistant models, we used the highly aggressive B16F10 murine melanoma model, known to be resistant to immunotherapy. For this resistant model, we used a total of eight IT injections of MVA-mIL-12 at 6×10^5 IFU. Mice treated with α PD-1 monotherapy succumbed to tumor burden and death within about 15 days (figure 1G). Treatment with MVA-mIL-12 significantly improved mice survival, alone and combined with α PD-1 compared with MVA empty (figure 1G). The therapeutic efficacy of MVA-mIL-12 was confirmed in a second CPI resistant model, the peritoneal CT26, refractory to the activity of α PD-1 (online supplemental figure 1C,D). These results highlighted that MVA-mIL-12 IT administration controls cancer progression as monotherapy and in combination with α PD-1, promoting antitumor activity in CPI sensitive and resistant models.

Local MVA-mIL-12 injection combined with α PD-1 exerts antitumoral activity on non-injected distant tumors

To test the abscopal antitumor response induced by MVA-mIL-12, bilateral tumor implantation models were used to evaluate whether treatment with MVA-mIL-12 could have antitumor activity also against distant, not injected tumors. IT injection of MVA-mIL-12 at the dose of 6×10^5 IFU or 10^7 IFU in combination with α PD-1 was performed in one of the masses of bilateral MC38 tumor bearing mice. In line with previous experiments, combination of α PD-1 and MVA-mIL-12 resulted at both doses in complete tumor regression of most injected tumors (figure 2A–C). Distant, not injected tumors were also eradicated on treatment in 50% and ~80% of animals, at the dose of 6×10^5 IFU and 10^7 IFU, respectively, underlying MVA-mIL-12 capability in controlling cancer growth at distant sites (figure 2D–F). Interestingly, the amount of murine IL-12 in distant tumors was very low compared with that one found in injected masses (figure 2G).

Intratumoral MVA-mIL-12 delivery remodels the TME from suppressive to pro-inflammatory

To elucidate the mechanism of action of MVA-mIL-12 and the impact on TME, we analyzed the immune composition of the MC38 TME by multicolor flow cytometry characterization. Briefly, MC38 tumor-bearing mice were treated with MVA-mIL-12 (6×10^5 IFU on days 0 and 4), α PD-1 or the combination of MVA-mIL-12 and α PD-1. MVA empty was used as control. On day 7, tumors were harvested and analyzed to characterize M1 pro-inflammatory macrophages, M2 anti-inflammatory macrophages, cDC1 and cDC2 DCs, NK cells, CD4 and CD8 lymphocytes. MVA-mIL-12, either alone or in combination with α PD-1, switches the TME from suppressive to pro-inflammatory with significant increase of the M1 pro-inflammatory macrophages, decrease of the M2 anti-inflammatory macrophages and recruitment of cDC1 cells (figure 3A–E). MVA-mIL-12 in combination with α PD-1 induces also a significant increase in CD8 and CD4 lymphocytes and a reduction of 50% in TREG, favoring a pro-inflammatory TME (figure 3G,H). No effect was instead observed on the levels of cDC2 (figure 3F), and NK (figure 3I). Moreover, on combined treatment with MVA-mIL-12 and α PD-1, IT CD8 T cells displayed increased cytotoxic markers,⁴⁰ such as augmented ability to produce IFN- γ and upregulation of CD69, and showed a memory phenotype (figure 3J).

The efficacy of MVA-mIL-12 in combination with α PD-1 was completely lost in BATF3^{KO} mice⁴¹ lacking cDC1 cells compared with control wild-type mice (figure 4A).

Antibody depletion studies to dissect the role of different immune cells in the MVA-mIL-12 mediated antitumor response showed loss of efficacy in CD8 and CD4 depleted mice (figure 4B), compared with isotype control treated mice. Instead, NK depletion did not affect MVA-mIL-12 efficacy (figure 4B).

These results were confirmed in the CT26 peritoneal metastatic model. Here, mice were treated IP with MVA-mIL-12 or MVA empty at day 0, 2 and 4 and groups of these mice were sacrificed at different time points. Treatment with both viruses caused at days 1 and 3 the complete disappearance of macrophages, known to encounter apoptosis after MVA infection^{42 43} (online supplemental figure 2A). Interestingly, at day 14, when macrophages were recruited again in the peritoneal cavity, they were M1 or M2 polarized in mice treated with MVA-mIL-12 or MVA empty, respectively (online supplemental figure 2B). MVA-mIL-12 induced an increase in DC compared with controls while no differences in cDC1 were observed in this model (online supplemental figure 2C). Also in this model, both CD8 and CD4 are essential for MVA-mIL-12 efficacy against cancer progression (online supplemental figure 2D,E). In addition, at day 14 a significant reduction in TREG cells was observed in the peritoneum of mice treated with MVA-mIL-12 compared with controls (online supplemental figure 2F). The key role of TME for the activity of MVA-mIL-12 is also suggested by the fact that intramuscular administration of

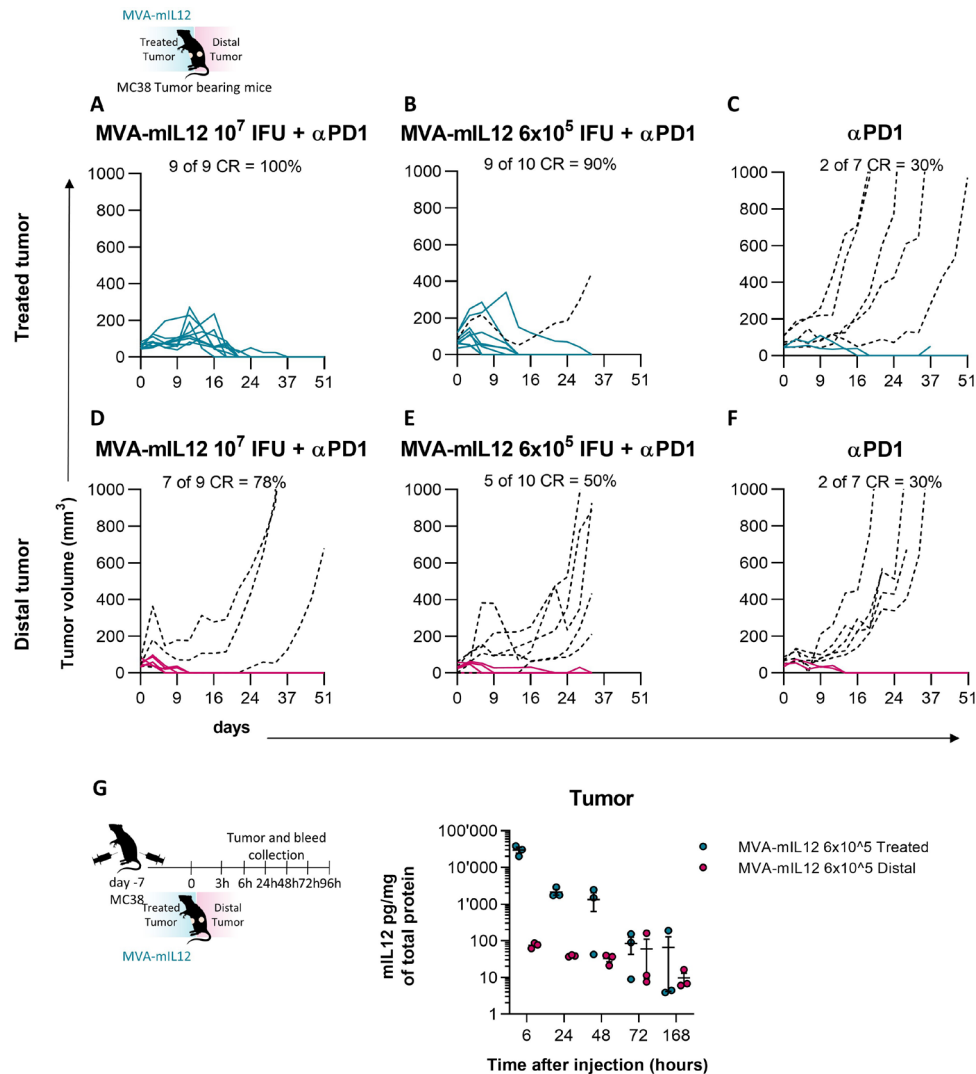


Figure 2 Local MVA-mIL-12 injection combined with α PD-1 exerts antitumoral activity on non-injected distant tumors. (A–F) C57BL/6 mice were challenged SC with MC38 cells on both flanks. After 7 days, mice with established tumors of similar volume were randomized. One tumor (treated) was injected IT with MVA-mIL12 at 10^7 IFU or 6×10^5 in combination with α PD-1 (A, B) the other one (distal) did not receive any IT treatment (D, E). Mice treated with α PD-1 only were used as control for both flanks (C, F). Tumor volume was monitored over time. Lines in the graphs represent each individual tumor (full lines, responder tumors; dot lines, non-responder tumors). Percentages on the graphs indicate the rate of complete response (CR). $n \geq 9$. (G) C57BL/6 mice were challenged SC with MC38 cells on both flanks. After 7 days, mice with established tumors of similar volume were randomized. One tumor (treated) was injected IT with MVA-mIL12 6×10^5 and the other one was left untreated (distal). ELISA was performed on both tumors: blue dots represent treated tumors, violet dots untreated ($n=3$). IFU, Infectious Unit; IL, interleukin; IT, intratumoral; m, murine; MVA, Modified Vaccinia virus Ankara; PD-1, programmed cell death protein-1; SC, subcutaneous.

the virus in MC38 tumor bearing mice, did not give any complete responders, compared with intratumoral injection (online supplemental figure 2G).

MVA-mIL-12 induces expansion and diversification of the intratumoral TCR repertoire and affects the TME signature

To explore whether MVA-mIL-12 induces changes on tumor TCR repertoire, we compared the TCR repertoire from bulk RNA-Seq of MC38 tumors in the different treatment groups. MVA-mIL-12 alone and in combination with α PD-1 induced the expansion and diversification of intratumoral TCR- β repertoire, with the major effect achieved in the combination group showing a 10-fold

higher counts of total TCRs compared with MVA empty treated mice and a more diverse repertoire (figure 5A,B). Transcriptional profiles of tumors from the different treatment groups were also evaluated by RNA-Seq. Tumor samples were harvested at day 7 from untreated, α PD-1, MVA empty (lower dose 6×10^5 , day 0 and day 4) and MVA-mIL-12 (lower dose 6×10^5 , day 0 and day 4) alone or in combination with α PD-1. Hierarchical clustering of the DEGs demonstrated that the major changes in gene expression compared with the untreated mice were induced on the combination of MVA-mIL-12 and α PD-1 treatment, followed by MVA-mIL-12 treatment and α PD-1

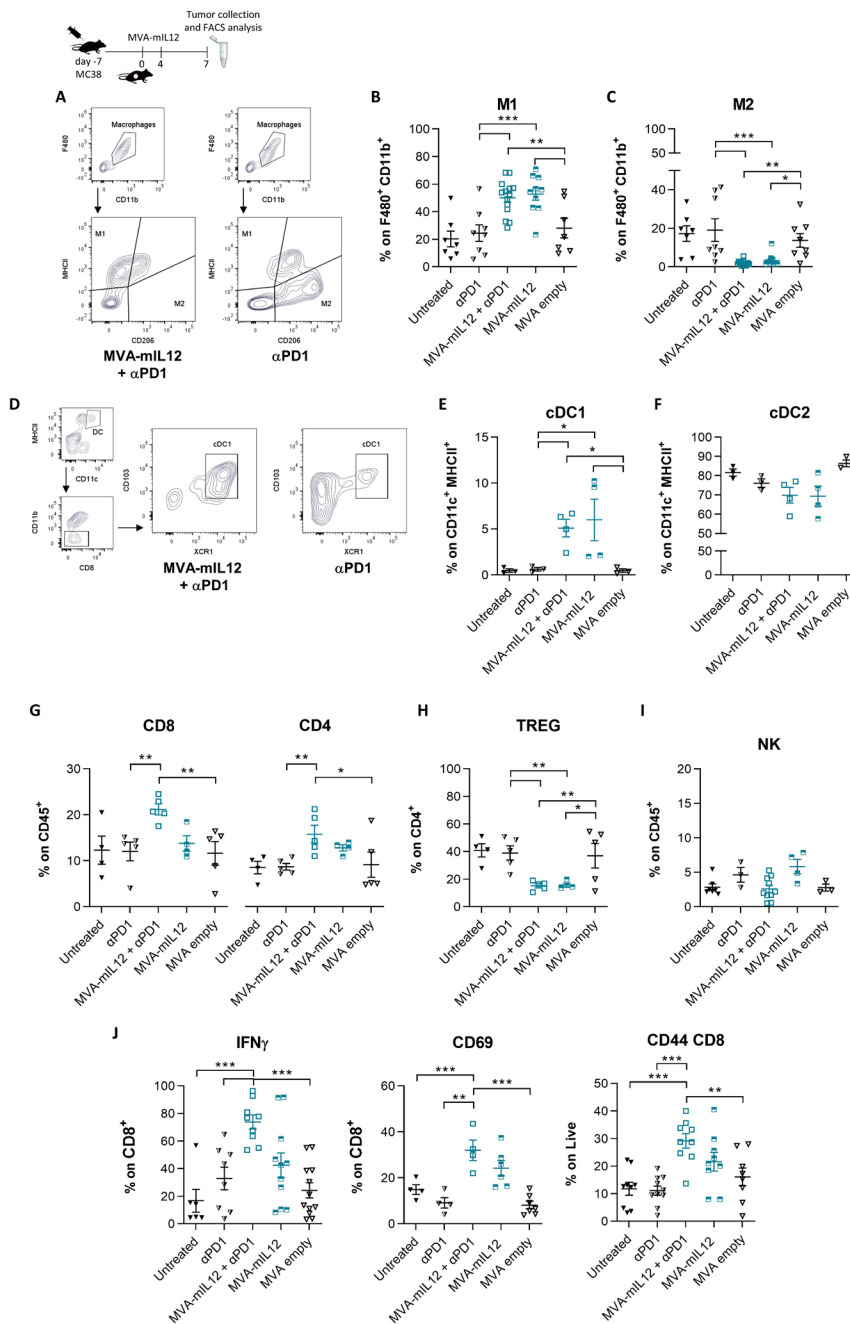


Figure 3 The TME is re-shaped by intratumoral treatment with MVA-mIL12. C57BL/6 mice were challenged SC with MC38 cells. After 7 days, mice with established tumors were randomized and treated IT as in the scheme with α PD-1, MVA-IL-12 at 6×10^5 IFU, the combination of MVA-IL-12 (6×10^5 IFU) with α PD-1 or with MVA empty (6×10^5 IFU). Tumors from all the groups were collected and analyzed by Flow Cytometry. $n \geq 3$. In (A) representative contour plot of macrophages subpopulations; in (B) the frequency of MHCII⁺ CD206⁻ M1 macrophages, in (C) CD206⁺ MHCII⁻ M2 macrophages; in (D) representative contour plot of cDC1; in (E) graph represents CD103⁺ XCR1⁺ cDC1, in (F) XCR1⁻ SIRP⁺ cDC2, in (G) CD8⁺ and CD4⁺ lymphocytes, in (H) TREG CD4⁺ FOXP3⁺, in (I) NK cells, in (J) CD8⁺ IFN- γ ⁺, CD8⁺ CD69⁺ and memory CD8⁺ CD44⁺ lymphocytes. Data are presented as median values+SEM; $n \geq 3$ mice. One-way ANOVA with the Fisher LSD test was performed to obtain p values. *, $p < 0.05$; **, $p < 0.005$; ***, $p < 0.001$. ANOVA, analysis of variance; cDC1, conventional type 1 DC; DC, dendritic cell; FACS, Fluorescence-Activated Cell Sorter; IFN, interferon; IFU, Infectious Unit; IL, interleukin; IT, intratumoral; LSD, least significant difference; m, murine; MHC, Major Histocompatibility Complex; MVA, Modified Vaccinia virus Ankara; NK, natural killer; PD-1, programmed cell death protein-1; SC, subcutaneous; TME, tumor microenvironment; TREG, Regulatory T cells.

(figure 5C). The combination of MVA-mIL-12 and α PD-1 significantly induced major changes in the expression of genes associated with antigen presentation (H2-Ab1), CD8 proliferation (Il7r), cytotoxic effector signature

(Gzmb, IFN- γ), DC (Clec7a), inflammatory cytokines and receptors (Ccl5, Nos2, Cxcl9), leukocyte motility (Itgb2) and macrophages and DC activation (CD86) (figure 5D and online supplemental figure 3A). These

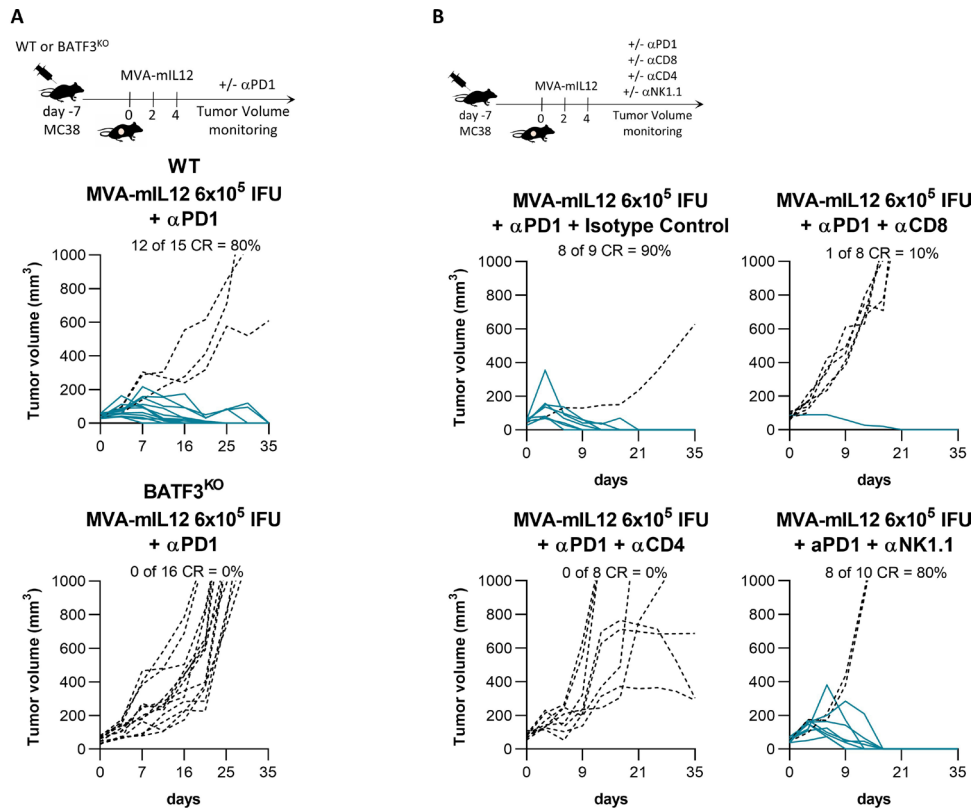


Figure 4 The efficacy of MVA-mIL-12 + αPD-1 is dependent on cDC1, CD4 and CD8. (A) C57BL/6 WT or BATF3^{KO} mice were challenged SC with MC38 cells. After 7 days, mice with established tumors were randomized and treated IT with MVA-mIL-12 (6×10⁵ IFU) and αPD-1. Lines in the graphs represent each individual tumor (full lines, responder tumors; dot lines, non-responder tumors). Percentages on the graphs indicate the rate of efficacy. (B) C57BL/6 mice were challenged SC with MC38 cells. After 7 days, mice with established tumors were randomized and treated IT with MVA-mIL-12 (6×10⁵ IFU) and αPD-1 in combination or not with isotype control, αCD8, αCD4 or αNK1.1 depletion antibody. Lines in the graphs represent each individual tumor (full lines, responder tumors; dot lines, non-responder tumors). Percentages on the graphs indicate the rate of efficacy. CR, complete response; IFU, Infectious Unit; IL, interleukin; IT, intratumoral; m, murine; MVA, Modified Vaccinia virus Ankara; NK, natural killer; PD-1, programmed cell death protein-1; SC, subcutaneous; WT, wild-type.

results support the increased intratumoral recruitment of macrophages and DC as well as T cells and their cytotoxicity in the MVA-mIL-12 with αPD-1 group.

MVA-mIL-12 reprograms the TME also of distant tumors

To gain a deeper understanding on the effect of MVA-mIL-12 on the distant uninjected tumors, we performed RNA-Seq by using the bilateral MC38 tumor models. Treated and distal tumor samples were harvested at day 7 from untreated and MVA-mIL-12 (dose 6×10⁵ IFU, day 0 and day 4) in combination with αPD-1. The expansion of intratumoral TCR clones was observed also in this context, in both treated and distal not injected tumors compared with untreated (figure 6A). Interestingly, common TCR clones in injected and uninjected tumors were identified on MVA-mIL-12 and αPD-1 treatment, suggesting induction of systemic antitumor immunity capable of mediating the regression of distal tumors (figure 6B), with a frequency of shared TCR between treated and distal tumors treated with MVA-mIL-12 and αPD-1 of 23% compared with 8% in the untreated group (figure 6C). Also here, the combination of MVA-mIL-12 and αPD-1 induced a high number of DEG with a

significant upregulation of genes in both treated and distal tumors compared with untreated controls (figure 6D). The analysis of DEG genes between treated and distal tumors versus the untreated controls displayed an overlapping set of genes in the two groups with an overlap of 38% (figure 6E). Among the common genes, we found increased expression of *Ccl5*, *Nos2*, *Cxcl9*, *Cxcl2*, *Gzmb*, *IFN-γ* in both treated and distal tumors, suggesting the acquisition of an immune-inflamed phenotype also in distant masses permissive for T-cell trafficking and activity (figure 6F,G).

DISCUSSION

TME represents a barrier for the development of effective cancer immunotherapies. The possibility to revert this immunosuppressive TME by using immune-activating cytokines is hampered by their toxicity on systemic administration. Here, we generated a non-replicative MVA encoding IL-12 for intratumoral delivery in a tight space-controlled and time-controlled manner, as strategy to turn ‘cold’ tumors into ‘hot’ tumors, while

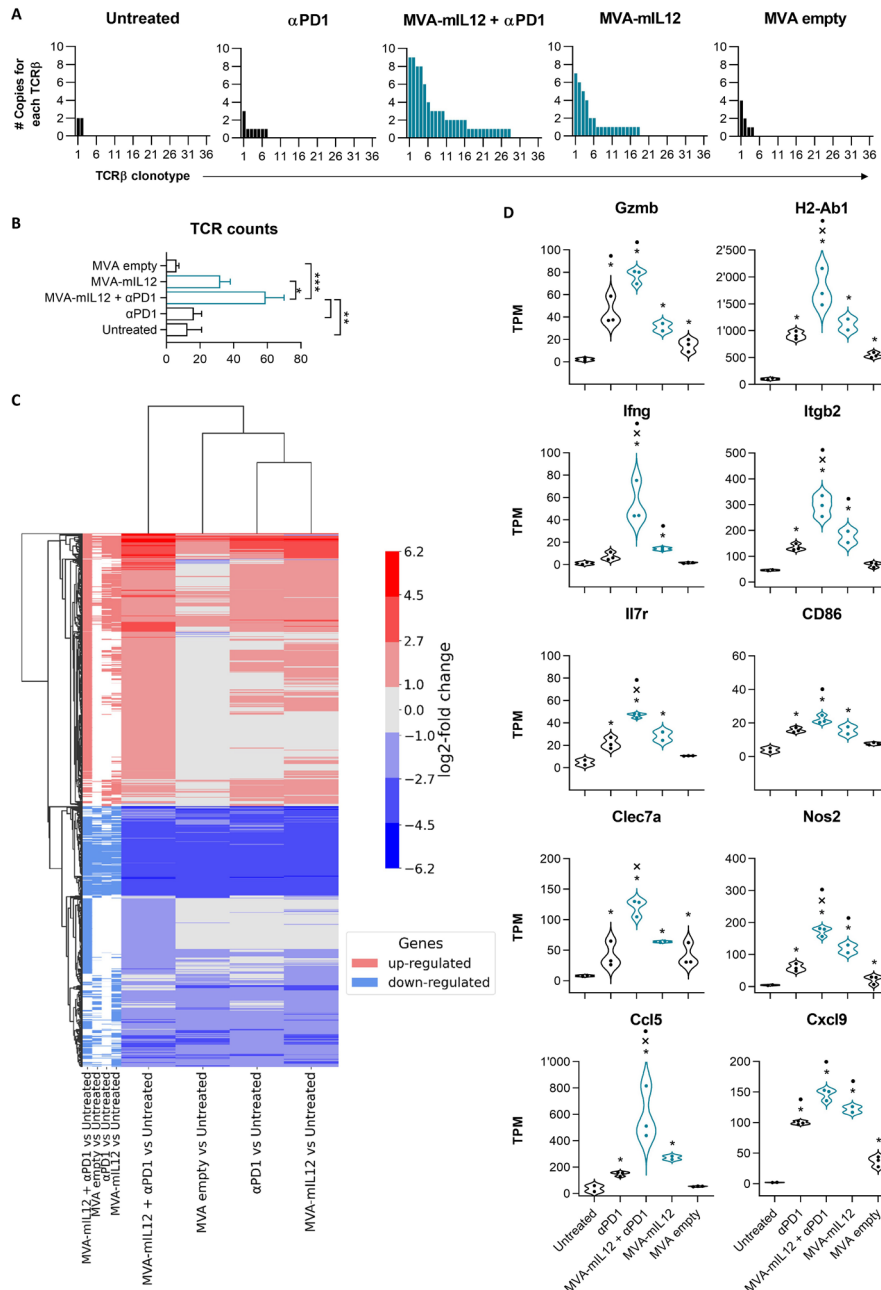


Figure 5 MVA-mIL-12 induces expansion and diversification of the intratumoral TCR repertoire and affects immune-related TME signature. MC38 tumor bearing mice were treated with MVA-IL-12 (6×10^5 IFU IT; d0, d4) with or without α PD-1, MVA empty, α PD-1 or left untreated. Tumors were harvested at day 7 and RNA-Seq was performed. (A) Bar charts reporting the number of TCR- β clones detected by RNA-Seq. Each bar represents a TCR- β individual clonotype. On the vertical axis the number of copies of each clonotype is reported. A representative mouse TCR- β repertoire for each group is shown. (B) Mean (+SEM) number of TCR clonotypes in each group ($n=3$). One-way ANOVA test with Fisher's LSD test was performed to obtain p value. *, $p < 0.05$; **, $p < 0.005$; ***, $p < 0.001$. (C) Heatmap representing the differentially expressed genes (red: up-regulated; blue: down-regulated) detected by RNA-Seq on tumors of mice for each group of treatment versus untreated ($n \geq 3$) (median log₂ fold change ≤ 1 or > 1 ; consensus of 3 methods; Benjamini-Hochberg corrected p value < 0.05). (D) Violin plots of select genes. Genes found differentially expressed when compared with untreated are indicated with an asterisk (*), while a cross (x), or a dot (·) indicates genes found differentially expressed versus α PD-1 and MVA empty, respectively. ANOVA, analysis of variance; IL, interleukin; IT, intratumoral; LSD, least significant difference; m, murine; MVA, Modified Vaccinia virus Ankara; PD-1, programmed cell death protein-1; TCR, T-cell receptor; TPM, Transcripts per Million; RNA-Seq, RNA sequencing.

sparing systemic adverse effects due to IL-12 circulating levels. This approach of 'Vector Aided Microenvironment Programming' couples the safety profile of the MVA and its pro-inflammatory properties with the strong

immunostimulatory function of IL-12. Intratumoral delivery of IL-12 by oncolytic viruses has been demonstrated to promote antitumoral response.⁴⁴ However, the effect of oncolytic viral therapy as well the expression of

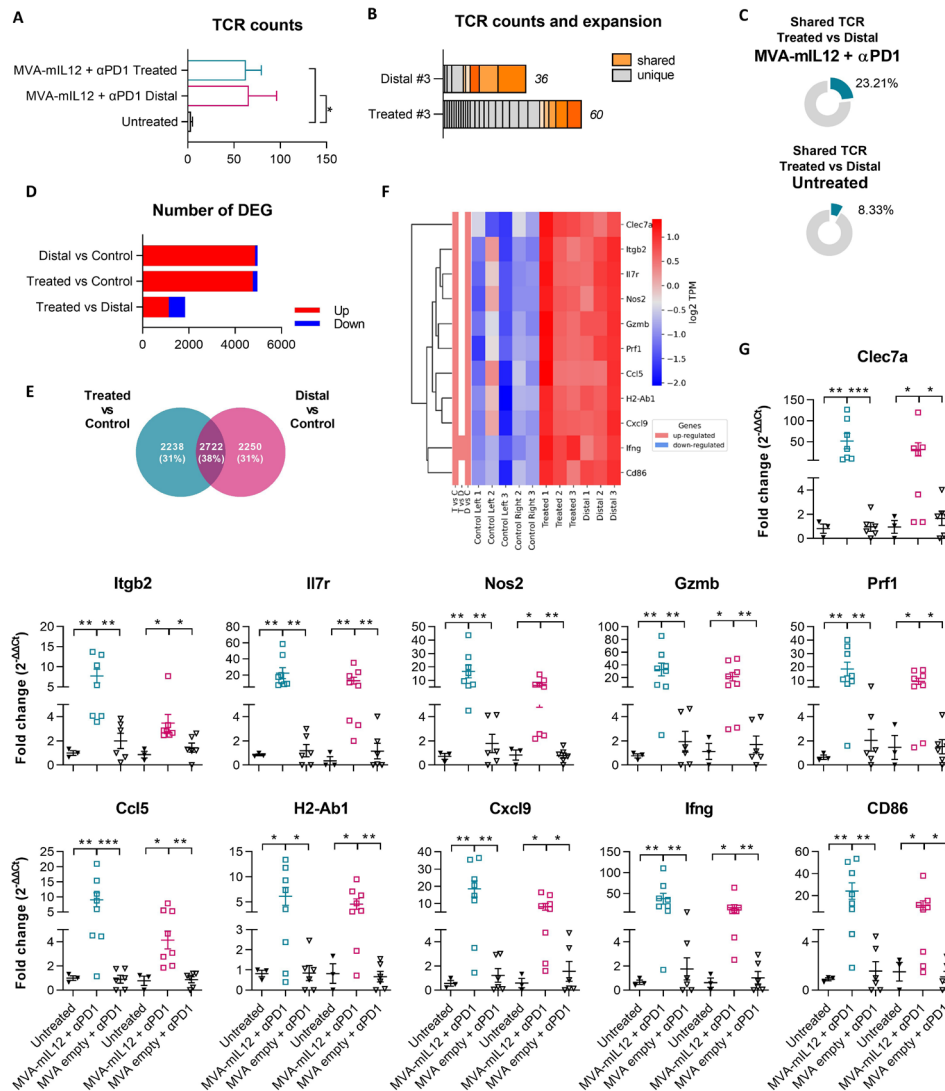


Figure 6 MVA-mIL-12 reshapes the TME of both treated and distant tumors. (A) Mean (+SEM) number of intratumoral TCR clonotypes in treated and distal MC38 tumors (bilateral tumor model) (n=3). Treated tumors were injected IT with MVA-mIL-12 at 6×10^5 IFU (d0, d4) in combination with α PD-1, while the distant tumors did not receive any IT treatment. One-way ANOVA test with Fisher's LSD test was performed to obtain p value. *, $p < 0.05$; (B) Representative bar chart reporting the total number of T-cell clones detected in treated and distal tumors. Shared clonotypes are represented with the same color. Gray clones are unique for each group. (C) Frequency of shared TCR between treated and distal tumors treated with MVA-mIL-12 and α PD-1 compared with the untreated group. (D) Bar chart showing the number of DEG (red: upregulated; blue: downregulated) detected by RNA-Seq on treated/distal tumors and untreated controls compared with each other. (E) Venn diagram displaying the overlap among the lists of DEGs obtained in each comparison. (F) Heatmap showing the expression values (TPM) of immune-related genes of interest detected in treated and distal tumors of mice receiving MVA-mIL-12 and α PD-1 versus untreated controls (left and right tumors). The annotation columns indicate DEGs in a specific comparison (median log₂ fold change of at least ± 1 ; consensus of three different methods Benjamini-Hochberg corrected p value in each method < 0.05). (G) MC38 bilateral tumor bearing mice were treated with the combination of MVA-mIL-12 and α PD-1, MVA empty and α PD-1 or left untreated. Treated and distal tumors were collected and analyzed by RT-PCR. One-way ANOVA test with Fisher's LSD test was performed to obtain p value. *, $p < 0.05$; **, $p < 0.005$; ***, $p < 0.001$. ANOVA, analysis of variance; DEG, differentially expressed gene; IFU, Infectious Unit; IL, interleukin; IT, intratumoral; LSD, least significant difference; m, murine; MVA, Modified Vaccinia virus Ankara; PD-1, programmed cell death protein-1; RNA-Seq, RNA sequencing; TCR, T-cell receptor; TME, tumor microenvironment; TPM, Transcripts per Million.

the encoded cargo relies on the infection and viral replication in cancer cells, which may be variable according to the tumor genotypes and not always guaranteed in all tumor cells.⁴⁵ In contrast, MVA is capable to infect and activate preferentially macrophages, DC, beside the cancer cells.⁴³ Moreover, MVA can encode therapeutic

molecules transiently and at high levels making the replicative capacity of the virus dispensable and therefore less risky both for the operator and for the patient. We showed that the treatment with MVA-IL-12 reprogrammed the TME towards a pro-inflammatory state while reducing pro-tumoral and immunosuppressive populations. Based

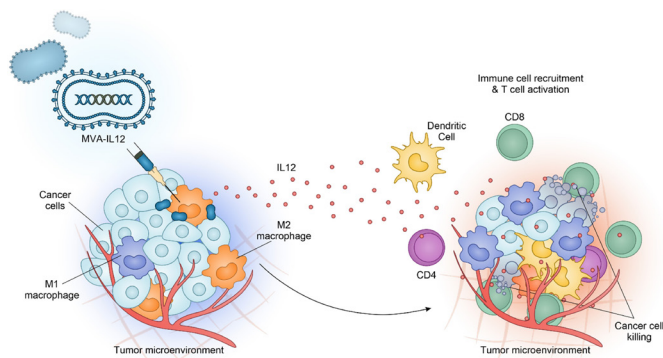


Figure 7 Working model of MVA-IL-12. Intratumoral administration of M-IL-12 resulted in TME reprogramming, reduction of immunosuppressive M2 macrophages while increasing pro-inflammatory M1, and recruitment of dendritic cells. This switch from immunosuppressive into immunostimulatory TME allows CD8 T cells to exert cytolytic activity against the tumor. IL, interleukin; MVA, Modified Vaccinia virus Ankara; TME, tumor microenvironment.

on our results, we proposed that intratumoral injection of MVA-IL-12 leads to localized IL-12 production by infected cells and induction of pro-inflammatory cytokines and chemokines in the TME (figure 7). This pro-inflammatory biased TME, favors polarization of M1 macrophages while reducing M2 macrophages, in line with the ability of IL-12 to convert TAM from suppressor macrophages into either inflammatory, pro-immunogenic macrophages.⁴⁶ M1 macrophages are themselves producers of IL-12 and chemokines such as CXCL9 and CXCL10 attracting DC and favoring T-cell priming. We have demonstrated herein that intratumoral injection of MVA-mIL-12 is able to induce potent antitumor immunity and worked in synergy with immune checkpoint blockade in multiple tumor models, including CPI resistant models. Importantly, MVA-mIL-12 combined to α PD-1 also promoted regression of untreated lesions in a dual flank MC38 model although the levels of IL-12 measured in distant tumors were much lower than the ones found in injected tumors. This suggests that the abscopal effects are likely due to trafficking from injected tumor to the distant one of cells of the innate immunity specifically activated in the injected tumor by MVA-mIL-12, in line with the acquisition of an immune-inflamed phenotype also in distant masses. This finally resulted in the expansion of intratumoral TCR clones observed in both treated and distal tumors and, more specifically, to the identification of shared clonotypes in both tumors. The ‘re-programmed’ TME is favorable to immune activation, allowing effective T cell mediated tumor cell killing, as demonstrated by the abolishment of the therapeutic activity after T-cell depletion and induction of T-cell memory supported by resistance of mice cured by MVA-mIL-12 to tumor re-challenge. Moreover, data in models resistant to α PD-1 activity support the hypothesis that MVA-mIL-12 might expand the utility of PD-1/programmed death-ligand 1 blockade to some patients resistant to CPI. It would be

of interest to further investigate the potential for other combination immunotherapies to synergize with MVA-mIL-12. One potential limitation for translation to the clinic could be the challenges posed by the intratumoral delivery. Intratumoral therapies need an accessible lesion for administration. However, image-guided technology might be used to target deep-seated lesions, and today increasing numbers of novel localized immunotherapy strategies and agents are currently pursued in clinic.⁴⁷ The translation plan and potential clinical applications of MVA-IL-12 are under investigation. The neoadjuvant treatment prior to tumor resection could be an ideal setting for clinical studies. Another indication of MVA-IL-12 could be the treatment of metastatic solid tumors in combinations with α PD-1 therapy in tumors resistant to immunotherapy, given our preclinical findings.

One aspect to be considered for clinical translation is the potential impact of anti-vector immunity for those subjects vaccinated against smallpox. Several clinical trials of recombinant MVA-based vaccines have shown that previous vaccination against smallpox had no effect on the development of an immune response to an MVA-administered antigen,^{48 49} suggesting that prior anti-vector immunity will not impede the effect of MVA-IL-12. Overall, our findings provide a strong rationale for exploring this approach in the clinic as a strategy to overcoming tumor resistance to immunotherapies.

Acknowledgements We acknowledge the animal facility of Plaisant in Castel Romano (Rome) for maintenance and care of the mice used in this study. We would like to thank in particular Domenico Salvatori for his support with tumor calibrations for *in vivo* studies.

Contributors Conceptualization: AMD, ES. Methodology: AMD, LS, LI, LN, MDL, GC, GL, EM, IG, GS, FT, SA, GR, LA. Investigation: LS, LI, LN, MDL, GC, GL, EM, IG, GS, FT, SA, GR. Visualization: AMD, ES, GL, LS, LN, MDL, IG. Funding acquisition: ES. Project administration: AMD, ES. Supervision: AMD, ES. Writing—original draft: AMD, LS. Writing—review and editing: ES. Guarantor: AMD.

Funding The authors have not declared a specific grant for this research from any funding agency in the public, commercial or not-for-profit sectors.

Competing interests ES is founder of Nouscom. AMD, LS, LI, LN, MDL, GC, GL, EM, IG, GS, FT, SA, GR are employees of Nouscom.

Patient consent for publication Not applicable.

Ethics approval Not applicable.

Provenance and peer review Not commissioned; externally peer reviewed.

Data availability statement All data relevant to the study are included in the article or uploaded as supplementary information.

Supplemental material This content has been supplied by the author(s). It has not been vetted by BMJ Publishing Group Limited (BMJ) and may not have been peer-reviewed. Any opinions or recommendations discussed are solely those of the author(s) and are not endorsed by BMJ. BMJ disclaims all liability and responsibility arising from any reliance placed on the content. Where the content includes any translated material, BMJ does not warrant the accuracy and reliability of the translations (including but not limited to local regulations, clinical guidelines, terminology, drug names and drug dosages), and is not responsible for any error and/or omissions arising from translation and adaptation or otherwise.

Open access This is an open access article distributed in accordance with the Creative Commons Attribution Non Commercial (CC BY-NC 4.0) license, which permits others to distribute, remix, adapt, build upon this work non-commercially, and license their derivative works on different terms, provided the original work is properly cited, appropriate credit is given, any changes made indicated, and the use is non-commercial. See <http://creativecommons.org/licenses/by-nc/4.0/>.

ORCID iDs

 Laura Secli <http://orcid.org/0000-0001-7129-3355>

 Linda Nocchi <http://orcid.org/0000-0002-2113-9031>

 Anna Morena D'Alise <http://orcid.org/0000-0002-0763-6269>

REFERENCES

- Schoenfeld AJ, Hellmann MD. Acquired resistance to immune checkpoint inhibitors. *Cancer Cell* 2020;37:443–55.
- Binnewies M, Roberts EW, Kersten K, et al. Understanding the tumor immune microenvironment (TIME) for effective therapy. *Nat Med* 2018;24:541–50.
- Labani-Motlagh A, Ashja-Mahdavi M, Loskog A. The tumor microenvironment: a milieu hindering and obstructing antitumor immune responses. *Front Immunol* 2020;11:940.
- Hinshaw DC, Shevde LA. The tumor microenvironment innately modulates cancer progression. *Cancer Res* 2019;79:4557–66.
- Bejarano L, Jordão MJC, Joyce JA. Therapeutic targeting of the tumor microenvironment. *Cancer Discov* 2021;11:933–59.
- De Lombaerde E, De Wever O, De Geest BG. Delivery routes matter: safety and efficacy of intratumoral immunotherapy. *Biochim Biophys Acta Rev Cancer* 2021;1875:188526.
- Trinchieri G, Rengaraju M, D'Andrea A, et al. Producer cells of interleukin 12. *Parasitol Today* 1993;9:97.
- Kobayashi M, Fitz L, Ryan M, et al. Identification and purification of natural killer cell stimulatory factor (NKSF), a cytokine with multiple biologic effects on human lymphocytes. *J Exp Med* 1989;170:827–45.
- Stern AS, Podlaski FJ, Hulmes JD, et al. Purification to homogeneity and partial characterization of cytotoxic lymphocyte maturation factor from human B-lymphoblastoid cells. *Proc Natl Acad Sci U S A* 1990;87:6808–12.
- Hsieh CS, Macatonia SE, Tripp CS, et al. Development of Th1 CD4+ T cells through IL-12 produced by listeria-induced macrophages. *Science* 1993;260:547–9.
- Manetti R, Parronchi P, Giudizi MG, et al. Natural killer cell stimulatory factor (interleukin 12 [IL-12]) induces T helper type 1 (Th1)-specific immune responses and inhibits the development of IL-4-producing Th cells. *J Exp Med* 1993;177:1199–204.
- Micallef MJ, Ohtsuki T, Kohno K, et al. Interferon-gamma-inducing factor enhances T helper 1 cytokine production by stimulated human T cells: synergism with interleukin-12 for interferon-gamma production. *Eur J Immunol* 1996;26:1647–51.
- Schmitt N, Bustamante J, Bourdery L, et al. IL-12 receptor beta1 deficiency alters in vivo T follicular helper cell response in humans. *Blood* 2013;121:3375–85.
- Valiante NM, Rengaraju M, Trinchieri G. Role of the production of natural killer cell stimulatory factor (NKSF/IL-12) in the ability of B cell lines to stimulate T and NK cell proliferation. *Cell Immunol* 1992;145:187–98.
- Kerkar SP, Goldszmid RS, Muranski P, et al. IL-12 triggers a programmatic change in dysfunctional myeloid-derived cells within mouse tumors. *J Clin Invest* 2011;121:4746–57.
- Steding CE, Wu S, Zhang Y, et al. The role of interleukin-12 on modulating myeloid-derived suppressor cells, increasing overall survival and reducing metastasis. *Immunology* 2011;133:221–38.
- Suzuki S, Umezū Y, Saijo Y, et al. Exogenous recombinant human IL-12 augments MHC class I antigen expression on human cancer cells in vitro. *Tohoku J Exp Med* 1998;185:223–6.
- Tugues S, Burkhard SH, Ohs I, et al. New insights into IL-12-mediated tumor suppression. *Cell Death Differ* 2015;22:237–46.
- Atkins MB, Robertson MJ, Gordon M, et al. Phase I evaluation of intravenous recombinant human interleukin 12 in patients with advanced malignancies. *Clin Cancer Res* 1997;3:409–17.
- Cirella A, Luri-Rey C, Di Trani CA, et al. Novel strategies exploiting interleukin-12 in cancer immunotherapy. *Pharmacol Ther* 2022;239:108189.
- Leonard JP, Sherman ML, Fisher GL, et al. Effects of single-dose interleukin-12 exposure on interleukin-12-associated toxicity and interferon-gamma production. *Blood* 1997;90:2541–8.
- Pittman PR, Hahn M, Lee HS, et al. Phase 3 efficacy trial of modified vaccinia Ankara as a vaccine against smallpox. *N Engl J Med* 2019;381:1897–908.
- Poland GA, Kennedy RB, Tosh PK. Prevention of monkeypox with vaccines: a rapid review. *Lancet Infect Dis* 2022;22:e349–58.
- Sutter G, Staib C. Vaccinia vectors as candidate vaccines: the development of modified vaccinia virus Ankara for antigen delivery. *Curr Drug Targets Infect Disord* 2003;3:263–71.
- Goepfert PA, Elizaga ML, Sato A, et al. Phase 1 safety and immunogenicity testing of DNA and recombinant modified vaccinia Ankara vaccines expressing HIV-1 virus-like particles. *J Infect Dis* 2011;203:610–9.
- Leoni G, D'Alise AM, Cotugno G, et al. A genetic vaccine encoding shared cancer neoantigens to treat tumors with microsatellite instability. *Cancer Res* 2020;80:3972–82.
- McCurdy LH, Larkin BD, Martin JE, et al. Modified vaccinia Ankara: potential as an alternative smallpox vaccine. *Clin Infect Dis* 2004;38:1749–53.
- Swadling L, Capone S, Antrobus RD, et al. A human vaccine strategy based on chimpanzee adenoviral and MVA vectors that primes, boosts, and sustains functional HCV-specific T cell memory. *Sci Transl Med* 2014;6:261ra153.
- Vollmar J, Arndt N, Eckl KM, et al. Safety and immunogenicity of IMVAMUNE, a promising candidate as a third generation smallpox vaccine. *Vaccine* 2006;24:2065–70.
- Lieschke GJ, Rao PK, Gately MK, et al. Bioactive murine and human interleukin-12 fusion proteins which retain antitumor activity in vivo. *Nat Biotechnol* 1997;15:35–40.
- Di Lullo G, Soprana E, Panigada M, et al. The combination of marker gene swapping and fluorescence-activated cell sorting improves the efficiency of recombinant modified vaccinia virus Ankara vaccine production for human use. *J Virol Methods* 2010;163:195–204.
- Kirchhammer N, Trefny MP, Natoli M, et al. NK cells with tissue-resident traits shape response to immunotherapy by inducing adaptive antitumor immunity. *Sci Transl Med* 2022;14:653.
- Ray A, Dittel BN. Isolation of mouse peritoneal cavity cells. *J Vis Exp* 2010:1488.
- Kim D, Paggi JM, Park C, et al. Graph-based genome alignment and genotyping with HISAT2 and HISAT-genotype. *Nat Biotechnol* 2019;37:907–15.
- Love MI, Huber W, Anders S. Moderated estimation of fold change and dispersion for RNA-Seq data with DESeq2. *Genome Biol* 2014;15:12.
- Sillar B, Plint CW. The price of a false-negative result of mammography and an overenthusiastic lay press. *Med J Aust* 1989;151:418.
- Law CW, Chen Y, Shi W, et al. Voom: precision weights unlock linear model analysis tools for RNA-seq read counts. *Genome Biol* 2014;15:R29.
- Tarazona S, Garcia-Alcalde F, Dopazo J, et al. Differential expression in RNA-Seq: a matter of depth. *Genome Res* 2011;21:2213–23.
- Liao Y, Smyth GK, Shi W. The R package rsubread is easier, faster, cheaper and better for alignment and quantification of RNA sequencing reads. *Nucleic Acids Res* 2019;47:e47.
- Kilinc MO, Aulakh KS, Nair RE, et al. Reversing tumor immune suppression with intratumoral IL-12: activation of tumor-associated T effector/memory cells, induction of T suppressor apoptosis, and infiltration of CD8+ T effectors. *J Immunol* 2006;177:6962–73.
- Kim TS, Gorski SA, Hahn S, et al. Distinct dendritic cell subsets dictate the fate decision between effector and memory CD8(+) T cell differentiation by a CD24-dependent mechanism. *Immunity* 2014;40:400–13.
- Garcia Z, Lemaître F, van Rooijen N, et al. Subcapsular sinus macrophages promote NK cell accumulation and activation in response to lymph-borne viral particles. *Blood* 2012;120:4744–50.
- Altenburg AF, van de Sandt CE, Li BWS, et al. Modified vaccinia virus ankara preferentially targets antigen presenting cells in vitro, ex vivo and in vivo. *Sci Rep* 2017;7:8580.
- Ge Y, Wang H, Ren J, et al. Oncolytic vaccinia virus delivering tethered IL-12 enhances antitumor effects with improved safety. *J Immunother Cancer* 2020;8:e000710.
- Zhang B, Wang X, Cheng P. Remodeling of tumor immune microenvironment by oncolytic viruses. *Front Oncol* 2020;10:561372.
- Watkins SK, Egilmez NK, Suttles J, et al. IL-12 rapidly alters the functional profile of tumor-associated and tumor-infiltrating macrophages in vitro and in vivo. *J Immunol* 2007;178:1357–62.
- Melero I, Castanon E, Alvarez M, et al. Intratumoural administration and tumour tissue targeting of cancer immunotherapies. *Nat Rev Clin Oncol* 2021;18:558–76.
- Harrop R, Connolly N, Redchenko I, et al. Vaccination of colorectal cancer patients with modified vaccinia Ankara delivering the tumor antigen 5T4 (TroVax) induces immune responses which correlate with disease control: a phase I/II trial. *Clin Cancer Res* 2006;12:3416–24.
- Cottingham MG, Carroll MW. Recombinant mva vaccines: dispelling the myths. *Vaccine* 2013;31:4247–51.